A Short-range Gradient of Histone H3 Acetylation and Tup1p Redistribution at the Promoter of the *Saccharomyces cerevisiae SUC2* Gene*

Abdelhalim Boukaba‡§¶, Elena I. Georgieva‡¶‖, Fiona A. Myers‡‡, Alan W. Thorne‡‡, Gerardo López-Rodas‡, Colyn Crane-Robinson‡‡, and Luis Franco‡§§**

From the ‡Department of Biochemistry and Molecular Biology, University of Valencia, Burjassot, E-46100 Valencia, Spain, ‖Institute of Genetics, Bulgarian Academy of Sciences, 1113 Sofia, Bulgaria, and ‡‡Biophysics Laboratories, Institute of Biomedical and Biomolecular Sciences, Faculty of Science, University of Portsmouth, Portsmouth PO1 2DT, United Kingdom

Chromatin immunoprecipitation assays are used to map H3 and H4 acetylation over the promoter nucleosomes and the coding region of the *Saccharomyces cerevisiae SUC2* gene, under repressed and derepressed conditions, using wild type and mutant strains. In wild type cells, a high level of H3 acetylation at the distal end of the promoter drops sharply toward the proximal nucleosome that covers the TATA box, a gradient that become even steeper on derepression. In contrast, substantial H4 acetylation shows no such gradient and extends into the coding region. Overall levels of both H3 and H4 acetylation rise on derepression. Mutation of *GCN5* or *SNF2* lead to substantially reduced *SUC2* expression; in *gnc5* there is no reduction in basal H3 acetylation, but large reductions occur on derepression. *SNF2* mutation has little effect on H3 acetylation, so SAGA and SWI/SNF recruitment seem to be independent events. H4 acetylation is little affected by either *GCN5* or *SNF2* mutation. In a double *snf2/gcn5* mutant (very low *SUC2* expression), H3 acetylation is at the minimal level, but H4 acetylation remains largely unaffected. Transcription is thus linked to H3 but not H4 acetylation. Chromatin immunoprecipitation assays show that Tup1p is evenly distributed over the four promoter nucleosomes in repressed wild type cells but redistributes upstream on derepression, a movement probably linked to its conversion from a repressor to an activator.

The *Saccharomyces cerevisiae SUC2* gene codes for invertase, an enzyme that catalyzes the hydrolysis of sucrose and raffinose to provide the cell with glucose in the absence of this essential fuel. It has been widely used to study the mechanisms underlying glucose regulation in yeast. Because these mechanisms result in changes in chromatin structure, this has been a long-lasting field of research. We first analyzed the DNase I sensitivity of the *SUC2* gene (1) as well as nucleosome positioning under repressing and derepressing conditions, in both wild type cells (2) and in regulatory mutants (3). These initial data, obtained by indirect end labeling, showed that four nucleosomes are positioned on the promoter in such a way that certain crucial elements, including the TATA box, are occluded, whereas other regulatory sequences are nucleosome-free (2). These results were refined by other workers (4, 5) who mapped the four nucleosomes at high resolution by primer extension analysis.

The *SUC2* gene is repressed in the presence of glucose by the Ssn6-Tup1 corepressor complex (6, 7), which is tethered to the promoter by Mig1p (8). Tup1-mediated repression of *SUC2* results in deacetylation of histone H3 at the promoter, as shown by an increase in H3 acetylation in *tup1* mutants, but a lack of Tup1p does not change the acetylation level of H4 (9). This result contrasts with findings for other Tup1-regulated genes in which the repression also results in deacetylation of H4 (9).

The *SUC2* gene is effectively derepressed by lowering the concentration of glucose (10), and several genes required for derepression were identified early through genetic screening (10, 11). These genes were collectively named *SNF* (sucrose non-fermenting). Further studies revealed that the *SNF* genes play two clearly different roles. The first is accomplished by the *SNF1* and *SNF4* genes. The former encodes a protein kinase (12), which acts in the pathway leading to *SUC2* derepression (13), whereas Snf4p regulates the kinase activity of Snf1p (14). The Snf1p kinase itself is rapidly phosphorylated in response to low glucose (15) and then, in turn, phosphorylates several proteins, including Mig1p (16). This seems to be a signal for the nucleus to cytoplasm translocation of Mig1p (17), and recent results seem to indicate that protein kinase C is also involved in this process (18). Importantly, translocation of Mig1p does not result in the release of Ssn6-Tup1, which remains bound to the *SUC2* promoter (19). The remaining *SNF* genes are involved in chromatin remodeling, as part of the SWI/SNF[1] complex as revealed by the pioneering studies of Hirschhorn *et al.* (20).

Derepression of *SUC2* also requires the action of the HAT

[1] The abbreviations used are: SWI/SNF, mating-type switching/sucrose nonfermenting; SAGA, Spt-Ada-Gcn5-acetyltransferase; YPD, yeast extract-peptone-glucose; X-ChIP, cross-linking/chromatin immunoprecipitation; wt, wild type; HAT, histone acetyltransferase.

activity of Gcn5p, as well as that of Ada2p and Ada3p (21). These proteins are components of the SAGA complex, which functionally interacts with the remodeling SWI/SNF complex (22). The participation of SAGA, which is largely specific for H3 (23) in *SUC2* derepression may explain observations that the level of H3 acetylation at its promoter increases in going from high to low glucose conditions (24).

Despite these data, many questions still remain concerning the mechanisms of *SUC2* derepression at a chromatin level. The precise role of the Ssn6-Tup1 complex in the activation of the gene and the relative roles of H3 and H4 acetylation in the process need clarification. Finally, the nature of the interactions between the SAGA and SWI/SNF complexes in the *SUC2* promoter are not yet clear. Because *SUC2* stands as a paradigm among the glucose-repressed genes in yeast, the answers to these questions are particularly important.

MATERIALS AND METHODS

Yeast Strains, Plasmids, and Media—The *gcn5* and *ada2* deletion mutants were obtained by appropriate gene disruptions of a parental strain with the genotype *MATα leu2Δ1 trp1Δ63 ura3–52*, further referred to as the wild type strain. All of these strains were kindly provided by G. Thireos. They are isogenic to the FY50, FY1291, FY1312, and FY1352 strains (*spt3*, *spt20*, *snf2*, and *gcn5snf2*, respectively), which were a gift from F. Winston. To construct the *gcn5ΔBr* mutant, lacking the bromodomain of Gcn5p, the *gcn5* deletion mutant was transformed according to the protocol of Ito *et al.* (25) with a centromeric plasmid bearing a truncated version of *GCN5* (26), which was also provided by G. Thireos.

Yeast cells were grown in a standard YPD medium (1% yeast extract, 2% bactopeptone, 2% glucose). To derepress *SUC2*, cells were transferred to a YPD medium containing low glucose (0.05%). For the growth of the mutant yeast cells, the YPD medium was supplemented with the required amino acids at the following concentrations (μg/ml): lysine, 40; histidine, 20; leucine, 60; tryptophan, 40; uracil, 20.

Formaldehyde Cross-linking and Chromatin immunoprecipitation—Cross-linking and immunoprecipitation of yeast chromatin was carried out by a modification of a previously published procedure (27). Cells harvested at mid-log phase ($A_{600} = 0.5$) were transferred to a conical flask, and formaldehyde (1% final concentration) was added. Cells were fixed at room temperature for 15 min under shaking, and the reaction was stopped by adding glycine to a final concentration of 0.125 M. The cross-linked yeast cells were collected by centrifugation and washed twice in ice-cold buffer containing 200 mM NaCl, 20 mM Tris-HCl, pH 7.5. The pelleted cells were then resuspended in 500 μl of ice-cold lysis buffer (150 mM NaCl, 1 mM EDTA, 1% Triton X 100, 0.1% SDS, 0.1% sodium deoxycholate, 50 mM Tris-HCl pH 8.0) supplemented with a mixture of yeast inhibitors of proteolytic enzymes (Sigma) and transferred to screw-top tubes. To homogenize the yeast cells, an equal volume of acid-washed glass beads (450–600 μm diameter) was added to each tube, and the cell suspensions were vortexed eight times at maximum speed for 1 min each. The tubes were kept on ice at least for 1 min between two consecutive vortexings. The homogenates were freed from the glass beads by washing four times with 500 μl of lysis buffer. The samples were then microfuged at 14,000 rpm for 10 min at 4 °C. The supernatants were discarded and the pellets resuspended in 1 ml of lysis buffer. To obtain soluble chromatin fractions, each sample was sonicated on ice 16 times, for 10 s each, at maximum power with a 3-mm microtip probe in a VC sonicator (Sonics & Materials, Inc.). All samples were chilled on ice for 2 min between sonications. In our hands, this sonication procedure yielded chromatin fragments with an average length of 350 bp, and fragments of more than 600 bp represented less than 15%. After sonication, the samples were microfuged at 14,000 rpm for 20 min at 4 °C. The pellets were discarded, and the supernatants were transferred to new tubes and centrifuged as described above. The final supernatants were frozen in liquid nitrogen and stored at −80 °C.

The following antibodies were used for ChIP assays: an affinity-purified polyclonal antibody recognizing the most highly acetylated forms of histone H3 (28), a polyclonal antibody specific for hyperacetylated histone H4 (29), and an affinity purified polyclonal anti-Tup1 antibody (30) kindly provided by A. D. Johnson.

For ChIP assays, the fixed chromatin solutions were cleared by stirring with protein A-Sepharose beads (25 μl of a 1:1 slurry) for 2 h at 4 °C. Before using, protein A-Sepharose was blocked with 0.1 μg/μl sheared λ DNA and 1 μg/μl bovine serum albumin for 4 h under rotation

at 4 °C. Precleared chromatin was divided into several fractions, transferred to new tubes, and incubated with 5 μl of anti-hyperacetylated histone H3 antiserum, 10 μl of the anti-hyperacetylated histone H4 antiserum, or 2 μl of anti-Tup1 antibody. Samples were rotated gently overnight at 4 °C, and 20 μl of protein A-Sepharose beads were then added to each sample and the suspensions incubated for an additional 2 h. Beads were recovered by centrifugation at 12,000 rpm for 1 min, the supernatants discarded, and the gel pellets resuspended in 1 ml of lysis buffer and rotated for 5 min at room temperature. Before the first washing of each sample, the supernatants from the reaction lacking primary antibodies were saved as input fractions and were processed together with the fractions eluted from the immunoprecipitates.

Immunoprecipitated chromatin was eluted from protein A-Sepharose in 100 μl of elution buffer (1% SDS, 100 mM NaH_2CO_3) at 65 °C for 10 min. The beads were re-extracted once more with 100 μl of elution buffer, and both eluates were pooled. Formaldehyde cross-linking was reversed by heating the eluates at 65 °C overnight. DNA from the eluates was purified by incubation with 100 μg/ml proteinase K at 37 °C for 1 h, extracted with phenolchloroform-isoamyl alcohol (25/24/1), precipitated overnight at −20 °C with 3 volumes of absolute ethanol in the presence of 1/10 (v/v) 3 M sodium acetate, pH 5.2, and 20 μg of glycogen as a carrier. DNA was recovered by centrifugation at 12,000 rpm for 15 min at 4 °C, washed twice with 70% ethanol, and dried in a SpeedVac for 5 min. The DNA obtained was then dissolved in 50 μl of TE buffer (1 mM EDTA, 10 mM Tris-HCl, pH 8.0) and saved at −20 °C for PCR analysis. The DNA from anti-Tup1 antibody immunoprecipitate was purified using Qiagen columns according to the manufacturer's instructions. DNA from all input and bound fractions was quantified with Pico Green (Molecular Probes) following the manufacturer's instructions.

PCR Analysis—Before PCR analysis (in a PerkinElmer 9600 thermocycler) of the immunoprecipitated samples, the linearity range for DNA amplification was determined by serial dilutions of each input and bound fraction. This showed that for immunoprecipitates with anti-H3 and anti-H4 antibodies, 1/10000-fold dilution of the input DNA and 1/50-fold of the bound DNA fractions followed by 30 cycles of PCR were appropriate. For the anti-Tup1 antibody immunoprecipitates, a 1/10000-fold dilution of the input, a 1/100-fold dilution of the bound DNA, and 26 cycles of PCR were used. PCR products were resolved on 2% agarose gels and quantified using Quantity One quantitation software (version 4, Bio Rad). The immunoprecipitation efficiency was calculated in triplicate according to Noma *et al.* (31). Briefly, the relative enrichment of H3 and H4 acetylation in the *SUC2* gene was estimated by dividing the amount of the PCR product from immunoprecipitated samples by the amount of the input sample prior to the immunoprecipitation. These *SUC2* ratios were then normalized for immunoprecipitation efficiency by dividing by the corresponding bound/input ratio for the *ACT1* (actin) gene PCR product.

Oligonucleotide PCR primers were designed to amplify segments within the four nucleosomes upstream of the start site of the *SUC2* gene and one segment near the middle of the coding region (see Fig. 2 for details). Oligonucleotide primers for the promoter region of the *ACT1* gene amplify a fragment from −156 to +45.

RNA Isolation and Northern Analysis—The hot acid-phenol method (32) was used to extract total RNA from 25 ml cell cultures. The RNA obtained was dissolved in sterile distilled water and its concentration was determined by measuring A_{260}. Total RNA (25 μg) from each sample was fractionated on a 1.2% formaldehyde agarose gel and blotted into a Hybond membrane (Amersham Biosciences) by capillary transfer. RNA was cross-linked by UV irradiation (254 nm) in a Bio-Rad apparatus. Hybridization was performed using Rapid-Hyb solution (Amersham Biosciences) for 1 h at 70 °C. All washes were done at 65 °C. The DNA probes for hybridization corresponded to positions +85 to +882 for *SUC2* and from +124 to +878 for *ACT1*. They were generated by PCR and labeled by random priming with [α-³²P]dCTP. Quantitation was performed with a FLA3000 Phosphoimager (Fujifilm) using the Image Gauge version 3.12 software.

Invertase Activity Analysis—Whole yeast cells from all strains and conditions used were grown to an A_{600} of 0.5 and collected by centrifugation, washed twice with cold distilled water, and resuspended to a concentration of 100 mg of cells/ml. Invertase activity was determined as described by Goldstein and Lampen (33) with the modifications of Celenza and Carlson (34). The invertase activity was expressed as μmol of sucrose hydrolyzed by the enzyme per min under standard assay conditions.
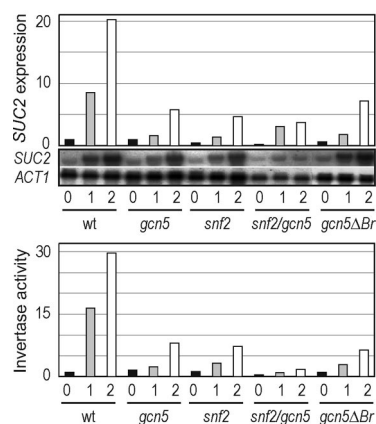
FIG. 1. **RNA expression analysis of the *SUC2* gene and invertase assays.** Yeast cells were grown in YPD medium under repressing conditions and then shifted to derepressing conditions. Aliquots from wt and mutant strains were taken at 0, 1, and 2 h, and total RNA was isolated and probed sequentially with *SUC2* and *ACT1* probes. Quantification of Northern blots was done using a Phosphoimager; the signals were normalized to the actin signal and plotted relative to noninduced wt as unity (*upper panel*). The *lower panel* shows the invertase activity assayed as described in the text and plotted relative to noninduced wt as unity.

RESULTS

RNA Expression Analysis of the SUC2 Gene in Wild Type and Mutant Strains—On shifting to low glucose concentration, *SUC2* is readily induced (derepressed). This system was used to examine the time course of expression levels in wild type yeast cells and in the mutant strains *gcn5, snf2, gcn5/snf2, ada2, spt3, spt20,* and *gcn5ΔBr.*

Fig. 1 (*upper panel*) shows the profile of *SUC2* mRNA expression. Set arbitrarily to 1 under basal conditions (wt 0 h), *SUC2* expression rises to 8 after 1 h in low glucose and to 20 at full derepression (2 h in low glucose). Under the same conditions, the *gcn5* mutant displays a severe phenotype; there is little change in the level after 1 h in low glucose, and it increases only 5-fold at 2 h. The *snf2* mutant shows a similar phenotype, which is in accordance with the involvement of *SNF2* in the expression of *SUC2*. The transcription rate of *gcn5ΔBr* mutant is roughly similar to that of the *gcn5* and *snf2* mutants, but the double mutant *gcn5/snf2* shows a very severe phenotype, and the expression of *SUC2* gene is almost negligible before induction and after 2 h of induction is similar to that of the repressed wt state. To evaluate the transcriptional rate in the double mutant, a correction for the expression level of the *ACT1* gene was required. In fact, an ~3.5-fold decrease in *ACT1* transcription was observed in the double mutants, in agreement with the data of Biggar and Crabtree (35). The expression of *ACT1* is not affected in single mutant strains, including *spt3* and *spt20*, which means that SAGA and other Gcn5p-containing HAT complexes are not involved in this effect. The results obtained in the invertase assay with some of the above mentioned strains (Fig. 1, *lower panel*) are in close agreement with the data on *SUC2* mRNA expression. It can thus be concluded that the expression of the *SUC2* gene in low glucose occurs to a very low extent in the *gcn5, snf2, gcn5/snf2, ada2, spt3, spt20,* and *gcn5ΔBr* mutants, and therefore, a repressing chromatin state may be expected in these mutants even under derepressing conditions. This conclusion agrees with our previous results with the *snf2* mutant (3).

High Resolution Mapping of Histone H3 and H4 Acetylation at the SUC2 Gene in Wild Type Cells—The acetylation state of histones H3 and H4 at the *SUC2* promoter was determined using the ChIP methodology combined with quantitative PCR as described under "Materials and Methods." Chromatin from
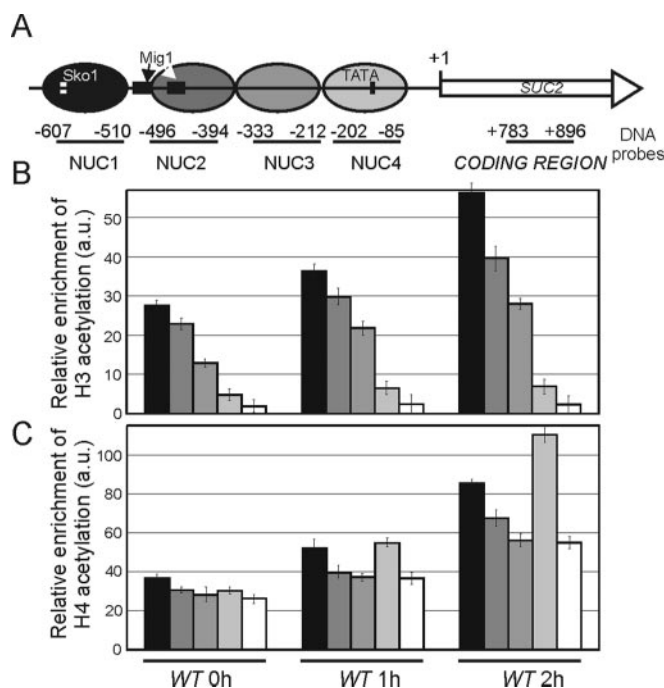

FIG. 2. **Relative enrichment in the acetylation of histones H3 and H4 (in arbitrary units (*a.u.*)) from wt cells after 0, 1, and 2 h induction.** *A*, map of the *SUC2* promoter showing the location of positioned nucleosomes (*ellipses*), certain relevant *cis* elements, and the PCR fragments amplified in the X-ChIP assays. The location of the PCR fragment from the coding region is also shown. *B* and *C* show the acetylation levels of H3 and H4, respectively, in the regions corresponding to each amplicon. *Bars* show mean ± S.E.

cross-linked yeast cells grown under repressing (0 h in low glucose) and derepressing conditions (1 and 2 h in low glucose) was sonicated and analyzed as described under "Materials and Methods." Fig. 2 gives enrichments for the four promoter and one coding amplicon. The upstream amplicons are short and correspond to the positions of the four promoter nucleosomes. Because the actual resolution is limited by the size of the fragments obtained after sonication, the *SUC2* coding sequences are probed with an amplicon located well downstream from the initiation site, at about the middle of the transcribed sequence, to avoid overlapping either with the *SUC2* promoter or with the gene that is of unknown function but constitutively expressed, which lies immediately downstream of *SUC2* (36). In the repressed gene, the level of H4 acetylation is roughly constant along the promoter and coding region, but the acetylation of H3 steadily decreases from the region of the distal nucleosome 1 to the coding region. Within the promoter itself, a 6-fold decrease is ongoing from nucleosome 1 to nucleosome 4. Upon derepression there is a general increase in H3 and H4 acetylation in the promoter. In the coding region the acetylation of H3 remains very low, but the substantial acetylation of H4 shows a 2-fold increase after 2 h in low glucose. The enrichment of H4 acetylation is roughly similar for nucleosomes 1 to 3 and in the coding region, but upon full derepression (2 h) a more pronounced hyperacetylation (more than a 3-fold increase over basal level) is observed centered on nucleosome 4, which lies over the TATA box.

High Resolution Mapping of Histone H3 Acetylation in the SUC2 Gene in the Mutant Strains—Fig. 3 shows the levels of H3 acetylation in the *gcn5, snf2, gcn5/snf2* and *gcn5ΔBr* mutants, as well as in the wild type strain. Results, given as histograms, are relative to the amount of acetylated H3 (taken as unity) in the repressed wild type cells. This normalization is to facilitate the comparison between wt and mutant strains at
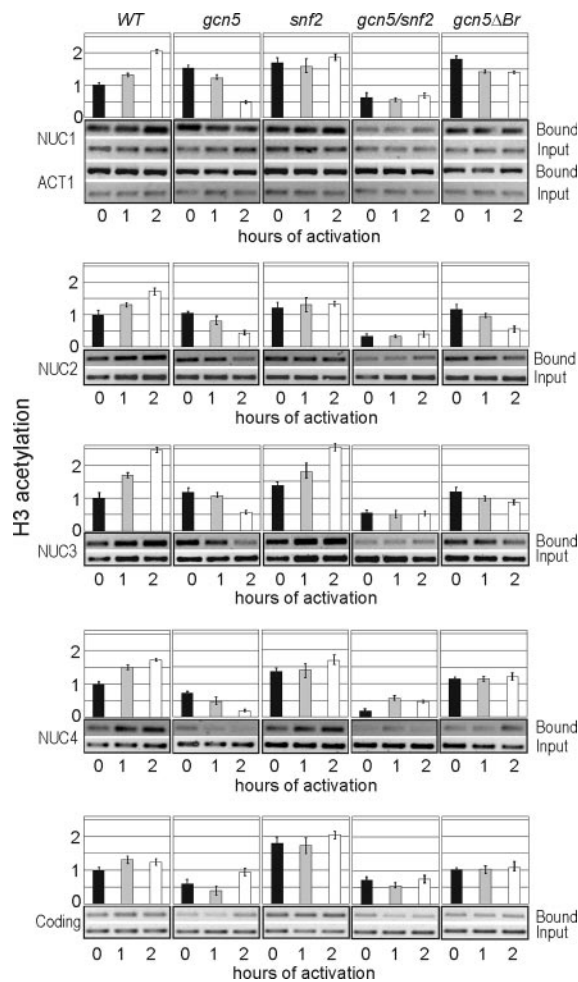
FIG. 3. **Histone H3 acetylation levels at the *SUC2* gene in wt and mutant strains.** X-ChIP assays were performed using the αAc-H3 antibody. DNA isolated from immunoprecipitated formaldehyde-cross-linked chromatin was subjected to PCR analysis using specific primer pairs encompassing positioned nucleosomes in the promoter and one fragment from the coding region (Fig. 2*A*) as well as a fragment from the actin promoter serving as a positive control for the ChIP assay. The histograms show the relative enrichments in acetylation, determined from the relationship (31) (bound *SUC2*/bound actin)/(input *SUC2*/input actin), where "bound" and "input" refer to the corresponding DNA fractions after immunoprecipitation and "*SUC2*" and "actin" stand for the amplicons used in the PCR analysis. Results are plotted relative to the value found in the repressed (0 h) wt cells for each amplicon. The gel bands resulting from the PCR analyses, as well as the input and actin controls, are shown below the histograms for each amplicon. The presence of acetylated H3 histone was assayed in wt, *gcn5*, *snf2*, *gcn5/snf2*, and *gcn5*ΔBr mutant strains.

each individual amplicon. In the *gcn5* mutant, the basal level of histone H3 acetylation is similar to that of the wild type strain and even somewhat higher in nucleosome 1. On the other hand, under derepressing conditions, a substantial decrease in histone H3 acetylation is observed along the entire promoter. These results indicate that the rise in histone H3 acetylation observed upon *SUC2* derepression in the wild type strain is dependent on Gcn5p, whereas the basal level observed in repressed cells is not. These comments do not apply to the coding region, where, after 2 h in low glucose, the level of histone H3 acetylation is similar to that in wild type cells.

In the *snf2* mutant, the basal level of histone H3 acetylation is higher than in the wild type along the entire *SUC2* locus. Moreover, H3 acetylation remains roughly constant over the 2 h of induction, in sharp contrast to the *gcn5* cells. The double mutant *gcn5/snf2* is characterized by a low level of H3 acetylation in both the promoter and the coding region, and this does
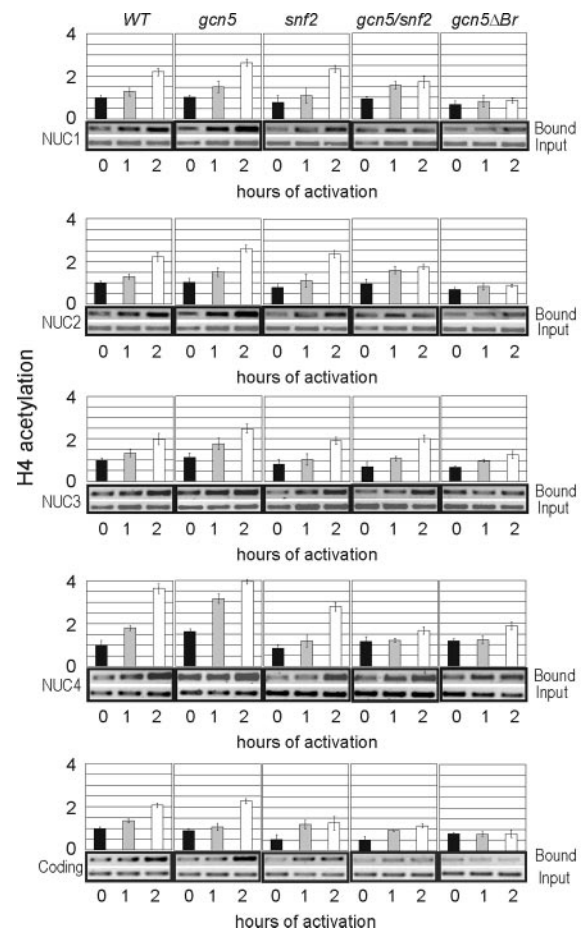

FIG. 4. **Histone H4 acetylation level at the *SUC2* gene in wt and mutant strains.** X-ChIP assays performed using an antibody against hyperacetylated histone H4, and the results are shown exactly as for acetylated H3 in Fig. 3.

not depend on the glucose concentration in the culture medium.

In the mutant strain *gcn5*ΔBr, there is little change in H3 acetylation ongoing from repressing to fully derepressing conditions. For nucleosome 1 the basal H3 acetylation is somewhat higher than in the *gcn5* mutant and drops slightly upon transfer to low glucose.

High Resolution Mapping of Histone H4 Acetylation in the SUC2 Gene in the Mutant Strains—Fig. 4 shows changes in H4 acetylation in *SUC2* promoter and coding region in the wt and four mutant strains. In the *gcn5* mutant the basal level of histone H4 acetylation in the promoter as well as in the coding region is almost identical to that in the wild type cells. Upon *SUC2* induction, the increase in H4 acetylation is similar to that in the wild type strain over the entire locus. The increase in H4 acetylation on the TATA box nucleosome, which becomes heavily acetylated in wild type cells (see Fig. 2), takes place even faster in the *gcn5* mutant (compare the wt and *gcn5* data at 1 h of derepression).

In the *snf2* mutant strain, the basal level of H4 acetylation over the entire *SUC2* locus is somewhat below that found in the repressed wild type. Nevertheless, significant increases are found after 2 h in low glucose, and the final levels generally match those found in wild type cells after 2 h induction (except, perhaps, for nucleosome 4). In contrast, the level of H4 acetylation in the coding region, although increasing 2-fold over its basal value on induction, still does not rise above the basal level found in wt and *gcn5* strains.

The *gcn5/snf2* double mutant shows H4 acetylation levels similar to wt under repressed conditions and on induction
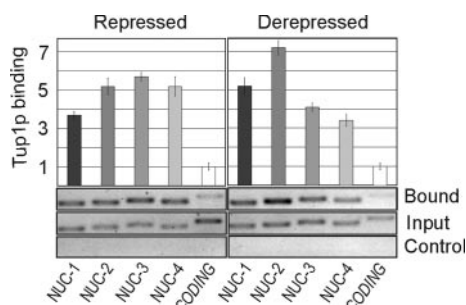
Histone Acetylation and Tup1p Binding in Yeast SUC2 Gene

FIG. 5. **ChIP assay of Tup1p occupancy at the *SUC2* promoter in WT.** Preparations of formaldehyde-cross-linked chromatin from wt strain with the *SUC2* gene, repressed (0 h) and fully derepressed (2 h in low glucose), were sonicated and immunoprecipitated by an anti-Tup1p antibody. Primer pairs within the four promoter nucleosomes and from the coding region (see Fig. 2) were used for quantitative PCR as described under "Materials and Methods." Tup1p binding at each amplicon was calculated by dividing the signal from the antibody-bound fraction by the signal from the corresponding input DNA. Aliquots from repressed and derepressed chromatin were treated in a similar way without antibody as a control.

increases 2–2.5-fold, rather as seen for the *snf2* strain and not so differently from wt cells. It is interesting to note that for this double mutant in which *SUC2* RNA levels are very much lower than in wt cells, the time-dependent pattern of H4 acetylation at the promoter is nevertheless similar to that of the wt strain, except in the region of the TATA box (nucleosome 4), where H4 acetylation remains approximately unchanged.

In the *gcn5ΔBr* mutant the H4 acetylation levels are similar to those of the *gcn5* mutant at nucleosome 1. At the other three nucleosomes and in the coding region, H4 acetylation levels are less than in *gcn5* and do not increase much on derepression, although mRNA levels and invertase activity in *gcn5ΔBr* are similar to those in the *gcn5* (Fig. 1).

Tup1p Mapping in the SUC2 Locus in the Repressed and Derepressed States—High resolution mapping of Tup1p occupancy in the *SUC2* gene (Fig. 5) revealed that when the *SUC2* gene is repressed, the Tup1p signal in the regions of nucleosomes 2, 3, and 4 is roughly constant, while somewhat smaller at nucleosome 1. In contrast, Tup1p is virtually absent from the coding region. Upon induction of *SUC2*, Tup1p remains bound to the promoter but a redistribution of the signal was observed, indicating a shift of the protein in the upstream direction. The Tup1p signal is now strongest in nucleosomes 2 and decreases in nucleosomes 3 and 4.

DISCUSSION

The sizes of the amplicons selected for the PCR analyses range from 97 to 127 bp and were selected to match the positioned nucleosomes of the promoter. The small size of the amplicons allowed acetylation and Tup1p mapping at a resolution limited only by the size of the chromatin fragments after sonication, which is on average 350 bp. This represents resolution at the dinucleosome level. Because in many cases the signal from amplicons in adjacent nucleosomes differs substantially, the implied differences in acetylation or Tup1p occupancy are presumably underestimated.

SUC2 Expression Levels—The present results show that the full expression of the *SUC2* gene depends upon the presence of intact SAGA and SWI/SNF complexes. In fact, the gene is incompletely derepressed (induced) upon shifting to low glucose in all of the studied strains bearing mutations in components of either the SAGA HAT complex (*gcn5, ada2, spt3,* and *spt20*) or the SWI/SNF remodeling complex (*snf2*). These results agree with previous reports (21, 22, 37), and the present experiment extends the study to other components of the above complexes. It is interesting to note that the bromodomain of

Gcn5p is required for full induction of the *SUC2* gene, because the increase in transcriptional rate under derepressing conditions in the *gcn5ΔBr* mutant is roughly similar to that in the strain lacking the whole *GCN5* gene (Fig. 1). On the other hand, a double mutation removing both the Gcn5p acetyltransferase activity and the remodeling activity of Snf2p results in the total unresponsiveness of *SUC2* to derepression by low glucose (Fig. 1).

Acetylation and Tup1p Occupancy in the wt Strain—A gradient of H3 acetylation is observed from the distal elements of the promoter to the coding region of the repressed *SUC2* gene in the wild type strain (Fig. 2), the acetylation of H3 being very low within the coding region. Upon derepression, the level of H3 acetylation in the coding region remains very low, but the gradient along the promoter becomes even sharper. This is in strong contrast to the distribution of acetylated H4, which spreads uniformly along the promoter and coding sequences in the repressed state but adopts a somewhat bimodal distribution upon derepression. In fact, the overall level of H4 acetylation increases along the whole *SUC2* locus upon shifting to low glucose, but the increase is particularly noticeable over the TATA box (nucleosome 4) and in the distal regions of the promoter (nucleosome 1).

There is a clear relationship between the level of histone acetylation and Tup1p occupancy. In the repressed gene, the Tup1p signal is spread over the four promoter nucleosomes (Fig. 5). The Ssn6-Tup1 complex is targeted to the promoter by the DNA-binding factor, Mig1p (8). There are two Mig1 sites in the *SUC2* promoter (38); the major one is at a GC-rich box located at −499, lying between nucleosomes 1 and 2, whereas the second site, of low affinity, is located at −442 within nucleosome 2 (Fig. 2). It is likely that the first site acts as an anchorage for the Ssn6-Tup1 complex via interactions with Mig1p in the repressed state. Although this site is almost 400 bp away from the TATA box, the Ssn6-Tup1 complex (a tetramer of Tup1 and a single Ssn6 subunit) has a very elongated shape as concluded from its hydrodynamic behavior (39), so it can readily extend toward nucleosomes 3 and 4. The physical interaction of Tup1p with Hos2p and Rpd3p histone deacetylases was described by Watson *et al.* (40) and a recent report from the same laboratory has established that multiple class I histone deacetylases, but not Hda1p, a class II enzyme, interact *in vivo* with both components of the corepressor complex (41). Tup1p shows a preferred interaction with hypoacetylated histone tails *in vitro* (42). If it behaves *in vivo* in the same manner, this would then contribute to generating a fixed repressed state, as suggested by Davie *et al.* (43).

Upon changing the medium to low glucose, Tup1p remains bound to the *SUC2* promoter (Fig. 5), in agreement with the recent data of Papamichos-Chronakis *et al.* (19). The high resolution analysis carried out in the present work allowed us to demonstrate that under derepression conditions there is a shift of the complex toward the distal regions of the promoter, because the maximal Tup1p signal is now found at nucleosome 2 (Fig. 5). In fact, the amplicon used by Papamichos-Chronakis *et al.* (19) in their Tup1 mapping corresponds to nucleosome 2 and some of nucleosome 1.

We propose the following mechanism to explain Tup1p displacement. First, under derepressing conditions, Mig1p is translocated to the cytoplasm (17) after being phosphorylated by the protein kinase Snf1p (16, 44). Then the corepressor complex Ssn6-Tup1 is converted into a coactivator; the shift between these two opposite functions of Ssn6-Tup1 has been described recently (19, 45). In stress-regulated promoters, this conversion of function involves the phosphorylation of Sko1p, the factor that tethers the corepressor complex to DNA, by the

mitogen-activated protein kinase Hog1p (45). It is interesting to note that in the *SUC2* promoter there is an Sko1 site upstream of the Mig1 high affinity site (46), which is shown in Fig. 2. If a mechanism similar to that acting on stress-regulated promoters is operative in the *SUC2* promoter, then the Ssn6-Tup1 complex would be retained in the derepressed state by interacting with phosphorylated Sko1p. This would explain the upstream displacement observed in the Tup1p signal upon derepression (Fig. 5). It has also been shown that Tup1p inhibits the binding of TBP at the *SUC2* promoter (47), and this could be why Tup1p moves away from nucleosome 4 on derepression.

It is worth noting that the movement of Tup1p relative to nucleosomes 1–4 might also result from a reorganization of chromatin rather than from actual Tup1-Ssn6 displacement. Promoter nucleosomes 2–4 are very closely packed (4, 5), so if remodeling results in an opening up of the promoter chromatin structure, a consequence could be reduced contact between the Tup1p complex and the TATA box region, whereas contact with Nuc1 and Nuc2 remains essentially unchanged.

Basal H3 Acetylation—The basal acetylation of H3 does not depend on Gcn5p-containing complexes (compare 0 h in the wt and *gcn5* panels of Fig. 3), in contrast to the derepression-induced acetylation of H3, which does require Gcn5p. This basal acetylation is high around the upstream activating sequence (Fig. 2), where a DNase I hypersensitive site exists (1). A relatively high, transcription-independent, basal level of histone acetylation is common in yeast (48), but the mechanisms for maintaining this nontargeted level of acetylation are not clear. Taking into account the correlation between histone hyperacetylation and DNase I sensitivity (49), it has been proposed that a causal relationship exists between these phenomena (50). It has also been suggested that the generation of an extended acetylated state in chromatin may involve the spreading of an initial acetylation event via the iterative recruitment of bromodomain-containing HATs (50). Nevertheless, this cannot be the mechanism operating to maintain the basal H3 acetylation in the present instance, because this level is maintained in the *gcn5ΔBr* mutant (Fig. 3). Although another component of the SAGA complex, Spt7p, also contains a bromodomain, this component is not involved in the anchorage of SAGA to acetylated nucleosomes (51).

Derepression-related Acetylation of H3 and H4—On derepression, our results indicate a recruitment of SAGA to the *SUC2* promoter, because in low glucose H3 acetylation increases in the promoter-bound histones (Figs. 2 and 3) in a Gcn5p-dependent manner (Fig. 3). These observations agree with those of other workers (19, 45) who have shown that the Ssn6-Tup1 complex, once converted into a coactivator, recruits the SAGA complex. Recruitment of the SAGA complex could displace the deacetylases from association with Tup1p in normal activation; however, in the absence of SAGA (*gcn5*) this loss of deacetylase would not occur, and the deacetylases could continue to remove acetylation from the promoter, as seen in the course of derepression with the *gcn5* mutant.

SAGA does not acetylate H4, and indeed, hyperacetylation of H4 in the *SUC2* promoter is independent of Gcn5p (Fig. 4). This means that a second HAT complex must be recruited to the *SUC2* promoter to account for the observed increase in H4 acetylation. NuA4 is the only H4-acetylating HAT complex described to date in yeast (52), but we have no data to ascertain the identity of the H4-acetylating complex recruited to the *SUC2* promoter.

Acetylation and Remodeling—The requirement for intact *SNF2* in the expression of *SUC2* (Fig. 1) is consistent with the known fact that, in addition to histone acetylation, an SWI/SNF-based remodeling of the promoter is also required for induction. However, in the absence of the remodeling ATPase Snf2p, acetylation of H3 at the *SUC2* promoter is largely unaffected (Fig. 3), an observation consistent with the idea that the recruitment of the SAGA complex does not depend on remodeling. H4 acetylation is similarly unaffected by the absence of Snf2p, and so the HAT complex responsible for its acetylation must also be recruited independently of remodeling activity. Even in the double *gcn5/snf2* mutant, there is little change in H4 acetylation at the promoter with respect to wt, but *SUC2* expression has fallen to very low levels. Overall, there is clearly no requirement for increased H4 acetylation anywhere in the promoter for derepression of *SUC2*.

Bromodomain Deletion of Gcn5p—In the absence of this module of the HAT, the transcriptional defects are somewhat less than when the whole protein is lacking (Fig. 1). This result agrees qualitatively with the previously reported effects of the Gcn5p bromodomain on the transcription of several genes (53–55). Although in the repressed condition the H3 acetylation in the bromodomain deletion mutant is similar to that when the whole of Gcn5p is absent, on derepression the H3 acetylation levels are maintained in the bromodomain mutant, unlike the situation in *gcn5*. This finding correlates with the observation that induced *SUC2* transcription is greater in *gcn5ΔBr* than in *gcn5*.

REFERENCES

1. Pérez-Ortín, J. E., Estruch, F., Matallana, E., and Franco, L. (1986) *Mol. Gen. Genet.* **205,** 422–427
2. Pérez-Ortín, J. E., Estruch, F., Matallana, E., and Franco, L. (1987) *Nucleic Acids Res.* **15,** 6937–6956
3. Matallana, E., Franco, L., and Pérez-Ortín, J. E. (1992) *Mol. Gen. Genet.* **231,** 395–400
4. Gavin, I. M., and Simpson, R. T. (1997) *EMBO J.* **16,** 6263–6271
5. Wu, L., and Winston, F. (1997) *Nucleic Acids Res.* **25,** 4230–4234
6. Williams, F. E., and Trumbly, R. J. (1990) *Mol. Cell Biol.* **10,** 6500–6511
7. Neigeborn, L., and Carlson, M. (1987) *Genetics* **115,** 247–253
8. Treitel, M. A., and Carlson, M. (1995) *Proc. Natl. Acad. Sci. U. S. A.* **92,** 3132–3136
9. Deckert, J., and Struhl, K. (2001) *Mol. Cell Biol.* **21,** 2726–2735
10. Carlson, M., Osmond, B. C., and Botstein, D. (1981) *Genetics* **98,** 25–40
11. Neigeborn, L., and Carlson, M. (1984) *Genetics* **108,** 845–858
12. Celenza, J. L., and Carlson, M. (1986) *Science* **233,** 1175–1180
13. Carlson, M., Osmond, B. C., Neigeborn, L., and Botstein, D. (1984) *Genetics* **107,** 19–32
14. Jiang, R., and Carlson, M. (1997) *Mol. Cell Biol.* **17,** 2099–2106
15. Wilson, W. A., Hawley, S. A., and Hardie, D. G. (1996) *Curr. Biol.* **6,** 1426–1434
16. Treitel, M. A., Kuchin, S., and Carlson, M. (1998) *Mol. Cell Biol.* **18,** 6273–6280
17. De Vit, M. J., Waddle, J. A., and Johnston, M. (1997) *Mol. Biol. Cell* **8,** 1603–1618
18. Salgado, A. P. C., Schuller, D., Casal, M., Leão, C., Leiper, F. C., Carling, D., Fietto, L. G., Trópia, M. J., Castro, I. M., and Brandão, R. L. (2002) *FEBS Lett.* **532,** 324–332
19. Papamichos-Chronakis, M., Petrakis, T., Ktistaki, E., Topalidou, I., and Tzamarias, D. (2002) *Mol. Cell* **9,** 1297–1305
20. Hirschhorn, J. N., Brown, S. A., Clark, C. D., and Winston, F. (1992) *Genes Dev.* **6,** 2288–2298
21. Pollard, K. J., and Peterson, C. L. (1997) *Mol. Cell Biol.* **17,** 6212–6222
22. Roberts, S. M., and Winston, F. (1997) *Genetics* **147,** 451–465
23. Grant, P. A., Eberharter, A., John, S., Cook, R. G., Turner, B. M., and Workman, J. L. (1999) *J. Biol. Chem.* **274,** 5895–5900
24. Bone, J. R., and Roth, S. Y. (2001) *J. Biol. Chem.* **276,** 1808–1813
25. Ito, J. C., Fukuda, Y., Murata, K., and Kimura, A. (1983) *J. Bacteriol.* **153,** 163–168
26. Syntichaki, P., Topalidou, I., and Thireos, G. (2000) *Nature* **404,** 414–417
27. Braunstein, M., Rose, A. B., Holmes, S. G., Allis, C. D., and Broach, J. R. (1993) *Genes Dev.* **7,** 592–604
28. Myers, F. A., Evans, D. R., Clayton, A. L., Thorne, A. W., and Crane-Robinson, C. (2001) *J. Biol. Chem.* **276,** 20197–20205
29. Torres, L., Ávila, M. A., Carretero, M. V., Latasa, M. U., Caballería, J., López-Rodas, G., Boukaba, A., Lu, S. C., Franco, L., and Mato, J. M. (2000) *FASEB J.* **14,** 95–102
30. Redd, M. J., Arnaud, M. B., and Johnson, A. D. (1997) *J. Biol. Chem.* **272,** 11193–11197
31. Noma, K., Allis, C. D., and Grewal, S. I. (2001) *Science* **293,** 1150–1155
32. Iyer, V., and Struhl, K. (1996) *Proc. Natl. Acad. Sci. U. S. A.* **93,** 5208–5212
33. Goldstein, A., and Lampen, J. O. (1975) *Methods Enzymol.* **42,** 504–511

34. Celenza, J. L., and Carlson, M. (1984) *Mol. Cell Biol.* **4,** 49–53
35. Biggar, S. R., and Crabtree, G. R. (1999) *EMBO J.* **18,** 2254–2264
36. Igual, J. C., González-Bosch, C., Franco, L., and Pérez-Ortín, J. E. (1992) *Mol. Microbiol.* **6,** 1867–1875
37. Recht, J., and Osley, M. A. (1999) *EMBO J.* **18,** 229–240
38. Bu, Y., and Schmidt, M. C. (1998) *Nucleic Acids Res.* **26,** 1002–1009
39. Varanasi, U. S., Klis, M., Mikesell, P. B., and Trumbly, R. J. (1996) *Mol. Cell Biol.* **16,** 6707–6714
40. Watson, A. D., Edmondson, D. G., Bone, J. R., Mukai, Y., Yu, Y., Du, W., Stillman, D. J., and Roth, S. Y. (2000) *Genes Dev.* **14,** 2737–2744
41. Davie, J. K., Edmondson, D. G., Cherie B. Coco C. B., and Dent, S. Y. R. (2003) *J. Biol. Chem.* **278,** 50158–50162
42. Edmondson, D. G., Smith, M. M., and Roth, S. Y. (1996) *Genes Dev.* **10,** 1247–1259
43. Davie, J. K., Trumbly, R. J., and Dent, S. Y. (2002) *Mol. Cell Biol.* **22,** 693–703
44. Lutfiyya, L. L., Iyer, V. R., DeRisi, J., DeVit, M. J., Brown, P. O., and Johnston, P. O. (1998) *Genetics* **150,** 1377–1391
45. Proft, M., and Struhl, K. (2002) *Mol. Cell* **9,** 1307–1317
46. Nehlin, J. O., Carlberg, M., and Ronne, H. (1992) *Nucleic Acids Res.* **20,** 5271–5278
47. Kuras, L., and Struhl, K. (1999) *Nature* **399,** 609–613
48. Vogelauer, M., Wu, J., Suka, N., and Grunstein, M. (2000) *Nature* **408,** 495–498
49. Hebbes, T. R., Clayton, A. L., Thorne, A. W., and Crane-Robinson, C. (1994) *EMBO J.* **13,** 1823–1830
50. Forsberg, E. C., and Bresnick, E. H. (2001) *BioEssays* **23,** 820–830
51. Hassan, A. H., Prochasson, P., Neely, K. E., Galasinski, S. C., Chandy, M., Carrozza, M. J., and Workman, J. L. (2002) *Cell* **111,** 369–379
52. Allard, S., Utley, R. T., Savard, J., Clarke, A., Grant, P., Brandl, C. J., Pillus, L., Workman, J. L., and Côté, J. (1999) *EMBO J.* **18,** 5108–5119
53. Marcus, G. A., Silverman, N., Berger, S. L., Horiuchi, J., and Guarente, L. (1994) *EMBO J.* **13,** 4807–4815
54. Candau, R., Zhou, J. X., Allis, C. D., and Berger, S. L. (1997) *EMBO J.* **16,** 555–565
55. Sterner, D. E., Grant, P. A., Roberts, S. M., Duggan, L. J., Belotserkovskaya, R., Pacella, L. A., Winston, F., Workman, J. L., and Berger, S. L. (1999) *Mol. Cell Biol.* **19,** 86–98